

platform, stabilization, drive and control

Stefan CHWASTEK

Cracow University of Technology, Institute of Machine Design
al. Jana Pawła II 37, 31- 864 Kraków, Poland
Corresponding author. E-mail: chwastek@mech.pk.edu.pl

**OPTIMAL STABILISATION OF PLATFORMS SUSPENDED BY ROPES
USING THE FREQUENCY CONVERTER CONTROL METHOD**

Summary. The ability to relocate the load from point A to B in the working space and within the specified time cannot be treated as an exhaustive definition of functional quality of modern cranes. Further requirements include the minimization of dynamic loading during the start-up and backing phase and vibration reduction through the control of drives. Besides, when 3D loads are to be handled, their position has to be stabilized. The objective function in this case becomes the minimal time of operation. This study provides a synthesis of an automatic control system for positioning and stabilization of the platform whilst in service.

**STABILIZACJA OPTYMALNA LINOWYCH PLATFORM PODWIESZANYCH
METODĄ STEROWANIA PRZEMIENNIKAMI CZĘSTOTLIWOŚCI**

Streszczenie. Zdolność do przemieszczenia ładunku z punktu A do punktu B przestrzeni roboczej w określonym czasie nie wyczerpuje pojęcia funkcjonalności współczesnej maszyny dźwigowej. Przeciwnie, wymaga się, aby poprzez sterowanie napędami minimalizować obciążenia dynamiczne w fazach rozruchu i hamowania jak również drgania przenoszonego ładunku. W przypadku przenoszenia ładunków przestrzennych dochodzi warunek stabilizacji położenia nosiwa. Jednocześnie funkcją celu jest minimum czasu operacji. W pracy przedstawiono syntezę układu automatycznej regulacji zapewniającego precyzyjne pozycjonowanie oraz stabilizację położenia poziomego platformy w czasie pracy.

1. INTRODUCTION

Eccentric position of the cog (centre of gravity) of the handled load with respect to the platform causes non-uniform loading of ropes supporting the platform. Forces acting in ropes impact on the motors of the lifting drives when acting upon the drums. The driving motor delivers the torque to match the loading moment, which is referred to as establishing the working point on the velocity characteristics. Depending on the static loading, the average rpm is established.

Asymmetry of the platform's loading is responsible for different tensioning of supporting ropes and, consequently, for differences in the loading of driving motors. As a result, ropes are wound on the drum at different rate, causing the platform to be inclined in the direction of the eccentric.

When the loads are to be lifted high, even minor differences in winding rate might lead to a disaster. When the platform loses its horizontal position, people standing upon or beneath are

exposed to danger from falling objects or spilling liquids. Another problem arises when large-sized housing elements are to be handled and assembled as it requires high-precision in positioning.

The purpose of this study is to develop an automatic control system to stabilize the platform in the horizontal position whilst in service and to ensure the precise positioning, in terms of reaching the required point on the trajectory within the specified period of time.

2. PHYSICAL MODEL OF A PLATFORM SUSPENDED ON ROPES

The physical model of the system comprising a platform suspended on two hoisting winches is shown in Fig 1. The number of DOFs of the system assumed to be planar equals 5, the flexibility of the driving systems being neglected (rigid couplings).

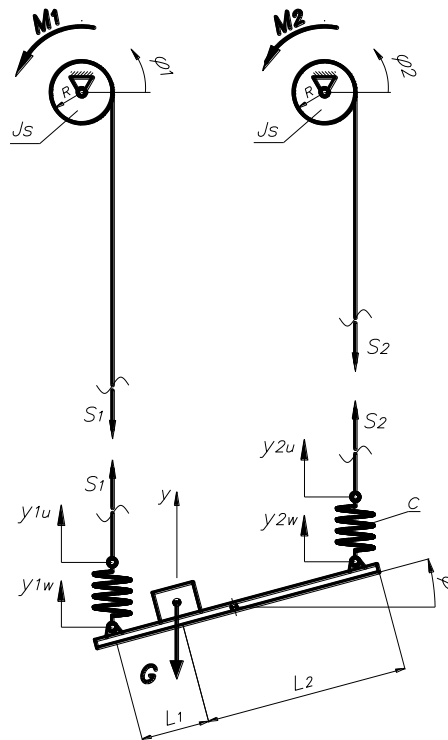


Fig. 1. Physical model of a platform suspended on a double-winch system
Rys. 1. Model fizyczny linowej, dwuciągarkowej platformy podwieszanej

Particular DOFs are represented by the elements of the vector of generalized coordinates $q(t) = [x(t), y(t), \varphi(t), \varphi_1(t), \varphi_2(t)]^T$. Horizontal vibrations being omitted, the planar motion of the platform as a rigid solid is described by the variables: $y(t), \varphi(t)$. Coordinates $\varphi_1(t), \varphi_2(t)$ represent angular excitations acting upon the drums and produced by driving motors.

Rope flexibility is proportional to its effective length (sag – l). Assuming the averaged value of the Young modulus $E = 125$ GPa for ropes with a non-metallic core, in accordance with [3], the modulus of elasticity of the rope is obtained from the formula:

$$c(l) = n \frac{EA}{l}, \quad (1)$$

where: A – effective cross-section area of the rope, n – multiplicity of the pulley block.

Damping in the ropes is assumed to be proportional to the modulus of elasticity through the dimensionless damping factor $\zeta_0 = 0,01$. The effects of rope tension on its stiffness and damping are neglected. Let us assume the rope model as shown in Fig 1, comprising a non-stretching rope section of the length equal to the current sag – l , complete with a spring with the stiffness $c(l)$.

The motion of the platform may therefore be treated as superposition of the hoisting motion caused by the non-stretching rope section being wound onto drums and of the relative movement of the platform's side edges with respect to the end sections of the rope being wound [1].

Vertical displacements of the winch-rope attachment points: y_1, y_2 are expressed as:

$$y_i(t) = \phi_i(t)r + y_{iw}(t) \quad i = 1, 2. \quad (2)$$

where: r – drum radius, y_{iw} – relative elongation of the i – th rope.

The mathematical model of a platform suspended on ropes can be expressed in the matrix format:

$$\mathbf{M} \cdot \ddot{\mathbf{q}} = \mathbf{F}_s + \mathbf{k} \cdot \dot{\mathbf{q}} + \mathbf{c} \cdot \mathbf{q} + \mathbf{Q}_f \cdot \mathbf{f}, \quad (3)$$

where: \mathbf{M} – inertia matrix; \mathbf{F}_s – vector of generalized static forces; \mathbf{c} – stiffness matrix; \mathbf{k} – damping matrix; \mathbf{Q}_f – matrix of control signals, \mathbf{f} – vector of control variables (frequency of control voltage) and $\mathbf{f} = [f_1, f_2]^T$.

Real systems often incorporate rope pulleys on booms mounted on top of buildings or other engineering structures so that gear motors with the drums should be integrated with the platform.

3. HOISTING WINCH MODEL

The driving unit typically incorporates a gear motor wherein the flange of an asynchronous a/c cage motor is bolted directly to the gear motor's housing. On the shaft in the gear motor is a drum.

The kinematics diagram of the driving unit (Fig. 2) reveals how mass and mass moment of inertia should be reduced.

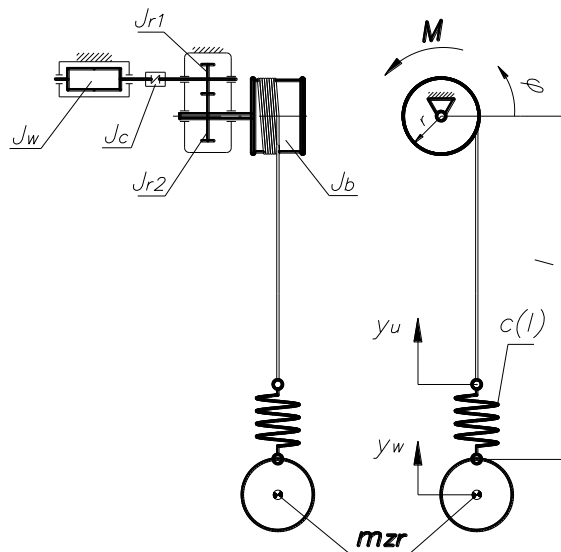


Fig. 2. Model of the driving unit in the hoisting winch
Rys. 2. Model układu napędowego wciągarki linowej

Torsional flexibility of the drive transmission system is neglected.

The gear motor can be integrated with an electric converter which controls the fluctuations of applied current supplying the induction motor in response to the control signals produced by the control system. The required output voltage signals can be achieved by several methods.

Controlling the speed of induction motors involves chiefly modulation of frequency of voltage fluctuations, which can be implemented using feedback loops in the electro-magnetic part of the system by the vector method, or alternatively, by the scalar method although with certain simplifications.

Application of the well-known *PWM* method (pulse width modulation) to the control of stator's current is a formidable task. In order to describe the electric power-supply system in a single wench it is required that eight differential equations are introduced, to handle the current flux and voltage flux in an asynchronous motor as well as those describing the converter [6].

Because of major reduction of the rpm, the predetermined hoisting rates are relatively small and the dynamic effects of the platform on the driving units in the winches are assumed to be insignificant.

Of particular interest, therefore, becomes the optimal frequency control strategy, based on steady-state characteristics of the motor.

The scalar method is applied here, based on a frequency converter to adjust the stator voltage U , proportional to frequency f , ensuring the stabilization of the magnetic flux [2].

Mechanical characteristics of an asynchronous induction motor controlled by adjusting the frequency of voltage supplying the stator winding, represented by the winch shaft, are shown in Fig. 3.

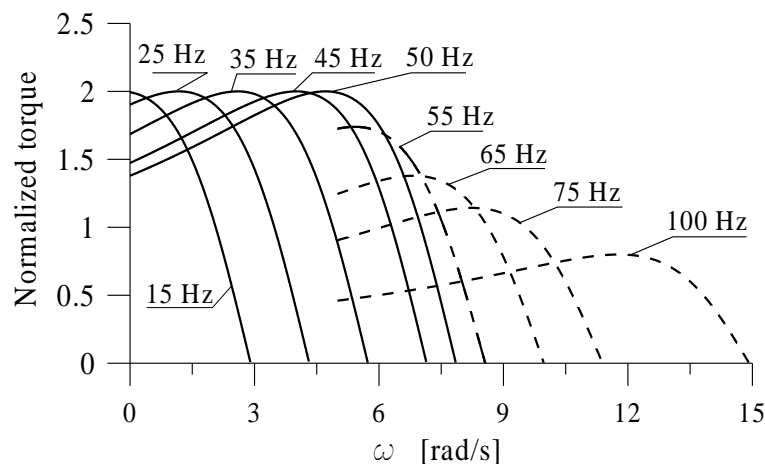


Fig. 3. Mechanical characteristics of an asynchronous induction motor controlled by adjusting the frequency of voltage supplying the stator winding, represented by the winch shaft

Rys. 3. Charakterystyki mechaniczne silnika indukcyjnego asynchronicznego sterowanego przez przemiennik częstotliwości z regulacją napięcia uzwojenia stojana zredukowane do wału wciągarki

Broken line designates motor loading characteristics collected at frequencies in excess of 50 Hz.

4. SYNTHESIS OF THE OPTIMAL CONTROL SYSTEM

Positioning of the platform can be regarded as a control problem in which the voltage frequency control is imposed in asynchronous motors $-f_s(t)$, and the motion of an object is thus determined to achieve the required trajectory. This is the leading signal forming the reference input $-f_s(t)$ in the control system, shown schematically in Fig. 5.

Fig. 4 shows a function of frequency fluctuation for the platform being elevated to the height 25 m within the time $T = 38$ s, taking into account a two-second start-up and backing phase during which

the hoisting speed varies sinusoidally and the passage through the steady state is assumed to be smooth. Besides, a two-second delay in the system's operation is assumed.

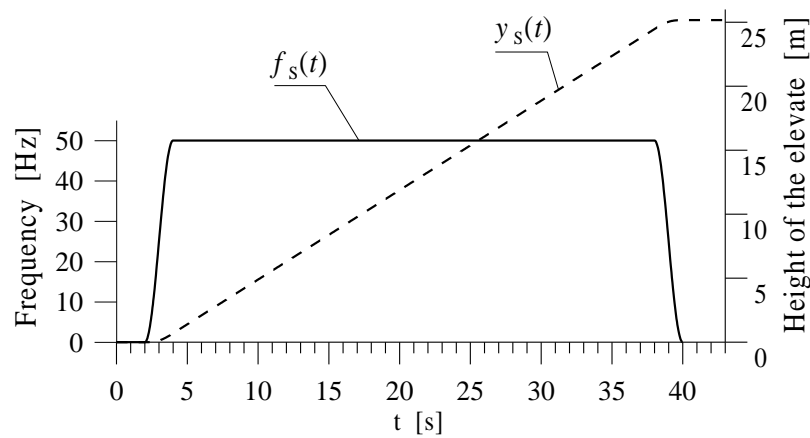


Fig. 4. Programmed frequency modulation of supply voltage $f_s(t)$ for the specified vertical displacement of the platform $y_s(t)$

Rys. 4. Programowo sterowana zmiana częstotliwości $f_s(t)$ napięcia zasilania dla planowanego pionowego przemieszczenia platformy $y_s(t)$

The designed control system in the space of states is governed by the equation:

$$\frac{d}{dt} \mathbf{z} = \mathbf{A}\mathbf{z} + \mathbf{B}\mathbf{u} + \mathbf{R}\mathbf{w}, \tag{4}$$

where: \mathbf{A} – matrix of state; \mathbf{B} – control matrix; \mathbf{R} – applied excitations matrix; \mathbf{w} – vector of applied excitations.

Among the variables of the vector of state $\mathbf{z} = [y, \varphi, \varphi_1, \varphi_2, \dot{y}, \dot{\varphi}, \dot{\varphi}_1, \dot{\varphi}_2]^T$, we select the measurement signals to generate vectors $\mathbf{y}(t)$. Comparing this vector to the vector of reference variables $\mathbf{y}_s(t)$ yields the control error [7].

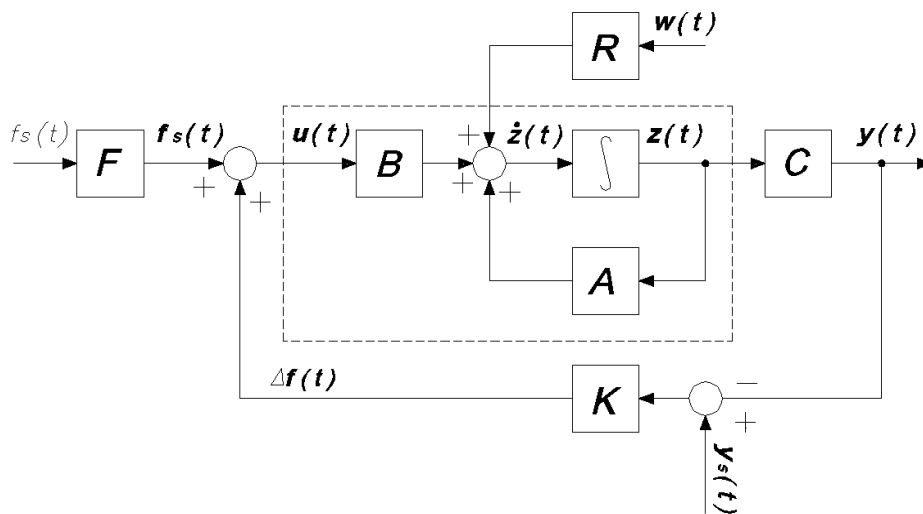


Fig. 5. Block diagram of an automatic control system with the reference input $f_s(t)$

Rys. 5. Schemat blokowy układu automatycznej regulacji z wejściem odniesienia $f_s(t)$

Synthesis of the optimal controller LQR requires that all variables of state should be observable. In the case considered here all variables of state are measurable, directly or indirectly, which implicates that the measurement matrix $C = I$.

The feedback signal from the state is generated in accordance with:

$$\mathbf{u}(t) = \mathbf{K} \cdot [\mathbf{z}_s(t) - \mathbf{z}(t)] + \mathbf{F} \cdot \mathbf{f}_s(t), \quad (5)$$

where: \mathbf{K} – desired feedback matrix; \mathbf{F} – forecast matrix.

The fact that the controllability and observability conditions can be satisfied proves the adequacy of the control strategy through frequency modulation of the supply voltage Δf_1 and Δf_2 .

The control quality criterion, utilising the sum of squared deviations of the state variables and control variables from the values resulting from the predetermined trajectory to be achieved within the specified period T , is expressed as a functional [4]:

$$J = \lim_{T \rightarrow \infty} \int_0^T [\mathbf{z}^T \mathbf{Q} \mathbf{z} + \mathbf{u}^T \mathbf{P} \mathbf{u}] dt, \quad (6)$$

where: \mathbf{Q} – weight matrix for the coordinates of state, \mathbf{P} – weight matrix for control.

In order to ensure the optimal control, represented by the minimum of the functional (6), it is required that the matrix \mathbf{X}_{opt} be determined, being the solution of the Riccati's differential equation:

$$\dot{\mathbf{X}}_{opt} + \mathbf{X}_{opt} \cdot \mathbf{A} + \mathbf{A}^T \cdot \mathbf{X}_{opt} - \mathbf{X}_{opt} \cdot \mathbf{B} \cdot \mathbf{P}^{-1} \cdot \mathbf{B}^T \cdot \mathbf{X}_{opt} + \mathbf{Q} = \mathbf{0}, \quad (7)$$

The optimal feedback matrix \mathbf{K}_{opt} is written as:

$$\mathbf{K}_{opt}(t) = -\mathbf{P}^{-1} \cdot \mathbf{B}(t)^T \cdot \mathbf{X}_{opt}(t). \quad (8)$$

5. PERFORMANCE OF THE CONTROL SYSTEM

Simulations were performed in Matlab-Simulink. For the platform 2 m in length loaded with the total weight $G = 4000$ N applied at the distance $L_1 = 0,7$ m from its left edge (as shown in Fig. 1), the error involved in positioning and leveling of the platform is shown in Fig. 6 and 7, respectively.

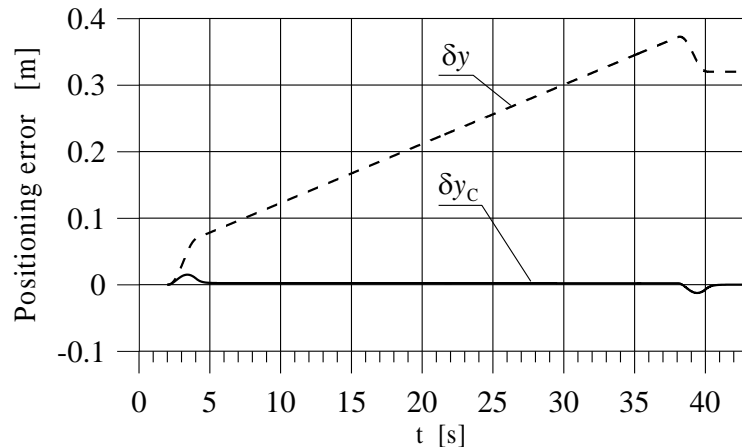


Fig. 6. Positioning error

Rys. 6. Uchyb pozycjonowania

Broken lines represent the control error whilst the platform is in service and the automatic control system is off, continuous lines represent the on-state of the automatic control system.

For the projected elevation of 25 m (see Fig. 5), the error in positioning control exceeds 0.3 m, while that involved in platform levelling equals 60° . When the platform is operated and the automatic control system is on, the positioning and levelling errors are nearly wholly eliminated.

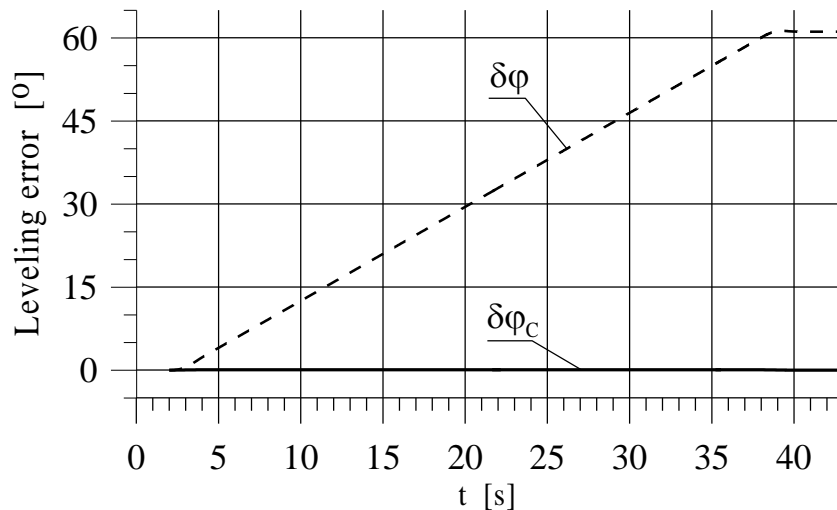


Fig. 7. Levelling error

Rys. 7. Uchyb poziomowania

The operation of the controller involves the frequency correction of voltage supplying the reference input, implemented by the feedback loop in the shape of signals Δf_1 i Δf_2 .

The variability range of correcting signals shown in Fig. 8 confirms that the proposed control method can be physically implemented.

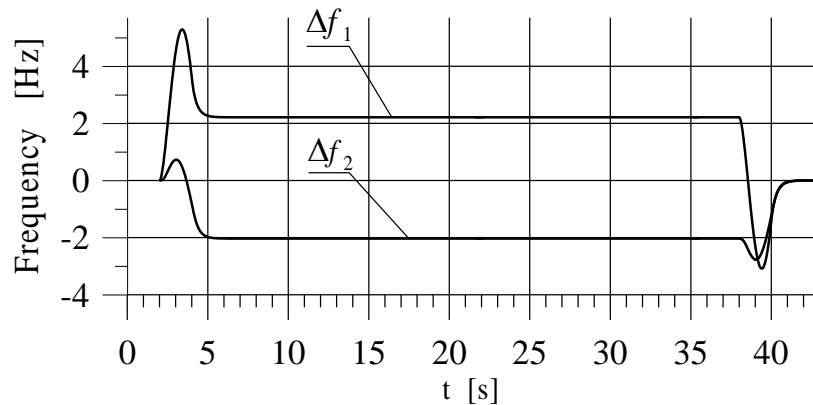


Fig. 8. Frequency correction

Rys. 8. Korekcja częstotliwości

6. CONCLUSION

In the context of minimizing the error involved in positioning and levelling of a suspended platform, the strategy for optimal modulation of frequency of voltage supplying the induction motors in the hoisting winches utilizes the scalar method of shaping the waveforms of output voltage signals.

Application of the scalar method is justified by limited dynamic interactions of the platform and the driving units.

Even though the model is simplified, especially its electro-magnetic part, the problem still remains nonlinear and non-stationary.

Results summarised in this study may be treated as reference for the application of vector methods.

Using the Simulink library, the simulation model is developed based on ready-made blocks of cage motors and *PWM* controllers. The “hold-up” moment effect is achieved at the zero rpm.

Control of motors is accompanied by major high-frequency oscillations of the time patterns of rpm, torque and forces acting in ropes, particularly during the start-up and braking phase.

In order that the method can be fully implemented, a thorough frequency analysis is required to explore the correlation between the frequency of natural vibrations of the mechanic system and the spectrum of the electro-magnetic moment. To handle highly dynamic processes, other vector methods are recommendable [9].

References

1. Cichocki W, Michałowski S.: *Laboratorium systemów transportu bliskiego i urządzeń dźwigowych. Część I. Budowa i badania*. Wydawnictwo PK. Kraków, 2011.
2. Tunia H., Kaźmierkowski M.: *Automatyka napędu przekształtnikowego*. WKiŁ, Warszawa, 1987.
3. PN – 90/B – 03200. *Konstrukcje stalowe. Obliczenia statyczne i projektowanie*.
4. Heimann B., Gerth W., Popp K.: *Mechatronika*. PWN, Warszawa, 2001.
5. Engel Z., Kowal J.: *Sterowanie procesami wibroakustycznymi*. Wydawnictwa AGH, 1995.
6. Dembowski A.: *Sposoby sterowania momentem w nowoczesnym napędzie elektrycznym*. Process Control Club 2001, poz.15, <http://pcc.imir.agh.edu.pl/poz15>
7. Rogalski A.: *Wpływ przekształtnika na moc znamionową trójfazowego silnika indukcyjnego*. Zeszyty problemowe – Maszyny elektryczne, Nr 78/2007, p. 137-146.
8. Chwastek S., Michałowski S.: *Stabilizacja optymalna osprzętu nieresorowanych maszyn na podwoziach kołowych*. Problemy Rozwoju Maszyn Roboczych, Zakopane, 2008, p. 41-42.
9. Dembowski A., Chudzik P, Lewandowski D.: *Napęd asynchroniczny ze sterowaniem momentu. Napędy i sterowanie*. Miesięcznik Naukowo-Techniczny Nr 4 (120), kwiecień 2009, p. 137-146.

Received 15.10.2010; accepted in revised form 23.10.2011